Structure–Property Correlation of a New Family of Organogelators Based on Organic Salts and Their Selective Gelation of Oil from Oil/Water Mixtures

Darshak R. Trivedi, Amar Ballabh, Parthasarathi Dastidar,* and Bishwajit Ganguly*[a]

Dedicated to Professor K. Venkatesan

Abstract: Organic salts based on dicyclohexylamine and substituted/unsubstituted cinnamic acid exhibit efficient gelation of organic fluids, including selective gelation of oil from an oil/water mixture. Among the cinnamate salts, dicyclohexylammonium 4-chlorocinnamate (**1**), 3-chlorocinnamate (**2**), 4-bromocinnamate (**3**), 3-bromocinnamate (**4**), 4-methylcinnamate (**5**) and the parent cinnamate (**6**) are gelators, whereas 2-chlorocinnamate (**7**), 2-bromocinnamate (**8**), 3-methylcinnamate (**9**), 2-methylcinnamate (**10**) and hydrocinnamate (**11**) are non-gelators. Non-gelation behaviour of **11** and various benzoate derivatives **12**–**18** indicate the significance of an unsaturated backbone in the gelation behaviour of the cinnamate salts. A structure–property correlation based on the single-crystal structures of most of the gelators (**1**, **3**, **5** and **6**) and non-gelators, such as **7**, **8**, **10**–**18**, indicates that the prerequisite for the one-dimensional (1D) growth of the gel fibrils is mainly governed by the 1D hydrogen-bonded network involving the ion pair. All the non-gelators show either two- (2D) or zero-dimensional (0D) hydrogen-bonded assemblies involving the ion pair. The molecular packing of the fibres in the xerogels of **1**, **3**, **5** and **6** has also been established on the basis of their simulated powder diffraction patterns, XRPD of bulk solids and xerogels. Ab initio quantum chemical calculations suggests that π–π interactions is not a contributing factor in the gelation process.

Keywords: ab initio calculations · aggregation · gels · hydrogen bonds · self-assembly · structure–property relationship

Introduction

Low-molecular-mass organic gelators[1–7] (LMOGs) are viscoelastic materials comprising an organic gelator and an organic liquid. LMOGs self-assemble into various types of aggregates, such as fibres, strands, and tapes, which are formed when a solution containing the gelator molecule is cooled below the gelation temperature (T_g). The aggregates are shown to cross-link among themselves through "junction zones"[8] to form a three-dimensional (3D) network that immobilises the solvent molecules and forms gels or viscous liquids. Unlike polymeric gels whose 3D network is based on covalent linkages, these physical gels obtained from LMOGs depend on relatively weak, non-bonded interactions, for example, hydrogen bonding, π–π stacking, and van der Waals interactions. Two distinct categories of gelators based on LMOGs, namely hydrogen-bond-based and non-hydrogen-bond-based gelators, are known according to the difference in the driving force for molecular aggregation. While polymeric gels are increasingly found in industrial applications, such as food, cosmetics, athletic shoes, and chromatography, LMOGs have also been found to be promising structure-directing agents (templates) to make helical transition-metal oxides[9] and silica,[10] to make microcellular materials,[5b] and in a CO_2-based coating process[5b] to make dye-sensitised solar cells.[11] Therefore, in recent years, studies on LMOGs have been an active research field in materials science and supramolecular chemistry. However, syntheses of LMOG have not become routine yet and many of them are serendipitous. It is also impossible to select a molecule that will definitely gel a selected liquid. Moreover, making most of such gelators involves non-trivial organic synthesis, and the design of these fascinating organic materials still remains a major challenge.

[a] D. R. Trivedi, A. Ballabh, Dr. P. Dastidar, Dr. B. Ganguly
Analytical Science Discipline
Central Salt & Marine Chemicals Research Institute
G. B. Marg, Bhavnagar - 364 002, Gujarat (India)
Fax:(+91) 278-567-562
E-mail: Parthod123@rediffmail.com
salt@csir.res.in

Supporting information for this article is available on the WWW under http://www.chemeurj.org/ or from the author. FT-IR data for **3**–**6**, **8**–**12**, ORTEP diagrams of **1**, **3**, **5**, **6**, **8**, **10**–**18**, crystal packing of **1**, **3**, **5**, **6** and **10**–**18**.

 DOI: 10.1002/chem.200400122

Our entry to the field of LMOG was rather serendipitous. While we were working on an area of crystal engineering based on organic acid–base adducts/salts,[12] we recently reported on the remarkable ability of a readily prepared organic salt to gel a few organic fluids.[13] Following this, we launched an extensive search for LMOGs based on organic salts and, in a recent communication, we revealed the discovery of the organic salts, namely dicyclohexylammonium 4-/3-chlorocinnamate (**1** and **2**, respectively) that are capable of gelling many organic fluids (polar, non-polar, edible oils and commercial fuels), including selective gelation of oil from oil/water mixtures.[14]

We have now undertaken systematic studies of related compounds (Scheme 1) and make an effort to formulate a

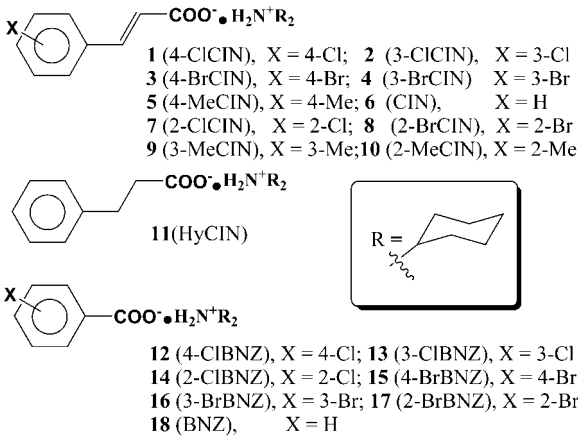

Scheme 1.

structure–property correlation. In so doing, we essentially attempt to address the major structural issues, namely: i) What, if any, is the relationship between the molecular packing of the bulk crystals of a molecule and its gelation behaviour? ii) How do the molecules pack in the fibres in the xerogel or gel state?

The answers to these questions will definitely provide valuable information that might help to decipher the mechanism of gel formation and eventually lead to the successful design of functional gelator molecules.

Herein, we report the syntheses of four new gelators, **3** (4-BrCIN), **4** (3-BrCIN), **5** (4-MeCIN) and **6** (CIN), as well as their gelation properties. A direct and straightforward structure–property correlation based on the single-crystal structures of the gelator molecules **1** (4-ClCIN), **3** (4-BrCIN), **5** (4-MeCIN) and **6** (CIN), and the non-gelators **8** (2-BrCIN), **10** (2-MeCIN), **11** (HyCIN) and **12**–**18** (all benzoate salts) has been achieved. To the best of our knowledge, this is one of the most clear-cut reports wherein a direct relationship between the hydrogen-bonding pattern in the crystalline state is correlated to the corresponding gelling or non-gelling property based on so many crystal structures of gelators and non-gelators, without any exceptions. Molecular packing of the primary assembly unit (fibres) in xerogels of **1** (4-ClCIN), **3** (4-BrCIN), **5** (4-MeCIN) and **6** (CIN) have also been established based on the XRPD of xerogels, bulk crystalline solids and single-crystal X-ray diffraction data. Since the cinnamic acid moiety contains a conjugated π system, we analysed the geometries obtained from ab initio quantum-chemical calculations, and, whenever possible, compared them with the corresponding crystal structures to probe the possible role of π–π interactions in the gelation process.

Results and Discussion

We concluded earlier, based on the crystal structure of **7** (2-ClCIN), that the position of Cl in the aromatic ring and the Cl···Cl interaction must play a role in the gelation process.[14] Therefore, we used bromo derivatives **3** (4-BrCIN), **4** (3-BrCIN) and **8** (2-BrCIN) for gelation studies. Both **3** (4-BrCIN) and **4** (3-BrCIN) are good gelators, whereas the corresponding 2-bromo-derivative **8** (2-BrCIN) appears to have no gelation ability. These results completely agree with our earlier observation on the corresponding chloro derivatives[14] and further support the observation that the position of the halogen in the ring must contribute to the gelation process. To make sure that this is indeed the fact, we studied derivatives without halogen substituents, such as **5** (4-MeCIN), **9** (3-MeCIN) and **10** (2-MeCIN) as well as the parent cinnamate salt **6** (CIN). To our surprise, we observed that **5** (4-MeCIN) and parent cinnamate salt **6** (CIN) also showed gelation behaviour. However, **9** (3-MeCIN) and **10** (2-MeCIN) failed to show any gelation ability with the solvents studied here. These results clearly indicate that even the methyl group at the 4-position and no substitution in the ring induce gelation in these cinnamate salts. To see whether the conjugated olefinic double bond in the cinnamic acid moiety plays a role in the gelation process, we also considered the corresponding saturated hydrocinnamate salt derivative **11** (HyCIN), halogen-substituted benzoate salts **12**–**17** and unsubstituted benzoate salt **18**. None of them showed any gelation properties with the solvents studied here, which indicates that the conjugated olefinic double bond in the cinnamic acid moiety must be one of the key features in this class of gelators.

Table 1 lists the gelation behaviour of **3**–**6**. Salt **3** (4-BrCIN) is able to rigidify non-polar and polar solvents as well as a few oils (commercial fuels and edible oils), whereas the corresponding 3-bromoderivative **4** (3-BrCIN) is only able to gel non-polar solvents and a few oils. The 4-methyl derivative **5** (4-MeCIN) is a good gelator capable of gelling most of the solvents listed in Table 1. On the other hand, the parent cinnamate salt **6** (CIN) does not appear to be as versatile gelator as its halogen or methyl derivatives.

To estimate the thermal stability of the gels of **1**–**5** in a common solvent *p*-xylene, a plot of the gel–sol dissociation temperature (T_{gel}) versus the gelator concentration was examined. Because **6** (CIN) is a less versatile gelator, it was not considered in this study. The increase of T_{gel} with the increase in gelator concentration (Figure 1) and also low minimum gel concentration indicates that self-assembly in the gel state is driven by strong intermolecular interactions.

Table 1. Gelation properties of **3–6**.

Entry	Solvent	**3** (4-BrCIN)		**4** (3-BrCIN)		**5** (4-MeCIN)		**6** (CIN)	
		MGC[c] [wt %][a]	T_{gel}[d]	MGC[c] [wt %][a]	T_{gel}[d]	MGC[c] [wt %][a]	T_{gel}[d]	MGC[c] [wt %][a]	T_{gel}[d]
1	CCl_4	2.85	65	–	ppt	–	ppt	–	FC
2	cyclohexane	0.75	72	–	FC	0.77	60	1.71	72
3	*n*-heptane	0.18	71	1.03	78	2.97	59	–	–
4	*n*-octane	–	VL	–	VL	0.52	87	–	FC
5	iso-octane	0.66	101	≤ 1	86	0.89	57	–	FC
6	*n*-decane	0.61	95	–	FC	1.05	76	–	FC
7	kerosene	0.66	92	2.23	85	–	FC	–	S
8	petrol	≤ 1	95	≤ 1	70	1.05	76	–	FC
9	diesel	0.22	104	–	S	–	FC	1.31	77
10	paraffin liq.	0.17	75	1.25	86	–	VL	–	VL
11	benzene	1.74	72	–	FC	0.95	53	–	ppt
12	toluene	0.65	76	5.43	70	0.60	70	–	FC
13	chlorobenzene	0.53	67	–	FC	1.17	63	–	FC
14	bromobenzene	0.71	70	–	FC	–	VL	–	FC
15	*o*-xylene	1.2	67	0.78	55	–	VL	–	FC
16	*m*-xylene	0.62	76	1.09	54	0.41	79	–	FC
17	*p*-xylene	1.08	80	0.54	56	1.08	80	–	FC
18	mesitylene	0.55	91	–	FC	1.12	73	0.73	68
19	methyl salicylate	1.99	65	–	S	–	VL	–	FC
20	1,2-dichlorobenzene	0.40	70	–	FC	1.08	57	–	FC
21	DMF	–	S	–	S	–	FC	–	ppt
22	ethyl acetate	0.45	57	–	ppt	–	FC	–	FC
23	DMSO	–	S	–	S	–	FC	–	S
24	nitrobenzene	0.29	73	–	S	0.40	65	–	FC
25	ground nut oil	0.60[b]	74	–	S	0.63	69	–	FC
26	cotton seed oil	0.58[b]	73	–	S	0.62	67	–	S
27	sunflower oil	0.19[b]	80	–	FC	0.74	74	0.94	55
28	coconut oil	0.20[b]	95	2.77	62	–	VL	1.65	65
29	1,4-dioxane	1.12	56	–	FC	2.04	43	–	–

[a] wt % = g per 100 mL of solvent. [b] g per 100 g of solvent. [c] MGC = minimum gelator concentration at room temperature. [d] T_{gel} = gel-to-sol dissociation temperature in °C; FC = fibrous crystal, VL = viscous liquid, S = solution; all gels are opaque and stable at room temperature for more than a month.

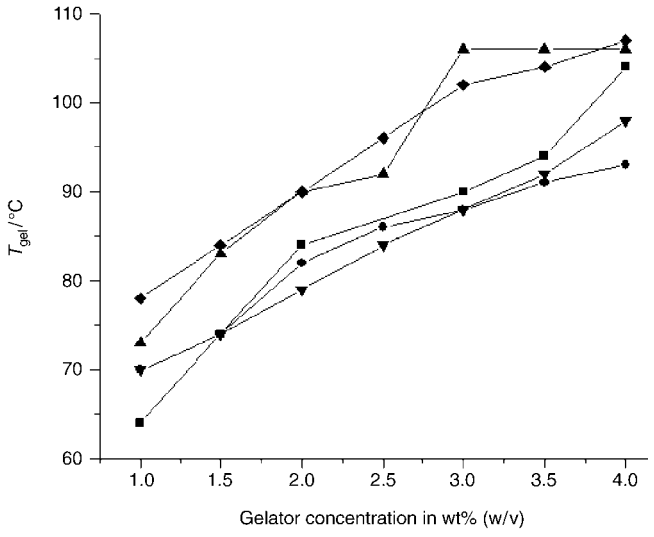

Figure 1. Plot of T_{gel} versus gelator concentration in wt % (w/v) in *p*-xylene for **1** (4-ClCIN) (▲), **2** (3-ClCIN) (▼), **3** (4-BrCIN) (■), **4** (3-BrCIN) (●) and **5** (4-MeCIN) (◆).

Selective gelation of oil from an oil/water mixture has recently been considered important for the containment of oil spills. [15] In our previous communication, we reported the remarkable selective gelation ability of **1** (4-ClCIN).[14] It is quite interesting that all the gelators, except **6** (CIN), are able to gel oil (either petrol or coconut oil) selectively in a biphasic mixture of oil/water (1 mL:1 mL). In a typical experiment, the gelator is added to a biphasic mixture of oil/water and heated either with or without a few drops of MeOH. The mixture is then allowed to cool to room temperature. After a few hours, the oil layer is found to be completely gelled leaving the water phase unaffected. The same observation is also seen when the experiments are conducted with vigorous shaking. While the petrol layer in a biphasic mixture of petrol/water is gelled by **2** (3-ClCIN), **3** (4-BrCIN), **4** (3-BrCIN) and **5** (4-MeCIN) (produces a viscous liquid in the absence of MeOH) either with or without a few drops of MeOH, the coconut oil layer was only gelled by **3** (4-BrCIN) without added MeOH. It may be noted here that, when the gelator is not soluble in water, gelation of oil from an oil/water mixture is not extraordinary and should not be called selective gelation in the true sense. In the present study, when the gelators (1.0 wt %) are left to equilibrate in a petrol/water mixture after heating the mixture at ~70 °C (remains biphasic), the water layer is found to contain 0.49 wt % **2** (3-ClCIN) (with and without MeOH), 0.45 wt % (with MeOH) and 0.23 wt % (without MeOH) **3**, 0.62 wt % **4** (3-BrCIN) (with and without MeOH) and 0.33 wt % (with MeOH) and 0.07 wt % (without MeOH) **5** (4-MeCIN). These results clearly show that the gelators are indeed soluble to a significant extent in the aqueous layer; however, they prefer to migrate into the oil layer resulting in its gelat-

ion. Therefore, it may be concluded here that the gelators (**2**–**5**) do show selective gelation properties.

SEM analyses of xerogels of **3**–**6** were performed to see the detail features of the fibres. Figure 2 depicts a typical 3D network of fibres in the xerogel of all the gelators studied here. FT-IR spectra of all the gelators as bulk solids, as solutions and as gels do not exhibit any shifts of the asymmetric stretching band of the COO- group (1641 cm^{-1}), which indicates that no additional hydrogen bonding is taking place during gel formation.

To address the important question as to what, if any, is the relationship between the molecular packing of the bulk crystals of a molecule and its gelation behaviour, we attempted structure–property correlation studies based on the single-crystal structures of most of the gelators and related non-gelator salts. According to recent reports by Shinkai et al. and collaborators,[16] 1D hydrogen-bonded network promotes gelation whereas 2D and 3D networks produce either a weak gel or do not promote gelation at all. If the plausible hydrogen bonding motif of secondary ammonium salts of monocarboxylic acid is considered, two main motifs, one 1D polymeric and the other cyclic zero-dimensional (0D) through N–H···O hydrogen bonding, can be envisaged[17] (Scheme 2).

Single crystals of gelators **1** (4-ClCIN), **3** (4-BrCIN), **5** (4-MeCIN) and **6** (CIN) were subjected to X-ray diffraction (Table 2). Interestingly, in the crystal structures of these gelators, hydrogen bonding through N–H···O interactions leads to the formation of a 1D network (Scheme 2 and Figure 3). It is also remarkable that, except **3** (4-BrCIN) (space group $P2_1/c$), the other gelators crystallise in the non-centric orthorhombic space group $P2_12_12_1$. The overall packing of the molecules in these cases appears to be close-packing of the T-shaped ion pair. It may be noted here that, in all these cases, the 1D hydrogen-bonded chains are packed in one direction, namely, down the crystallographic *a* axis (see the Supporting Information).

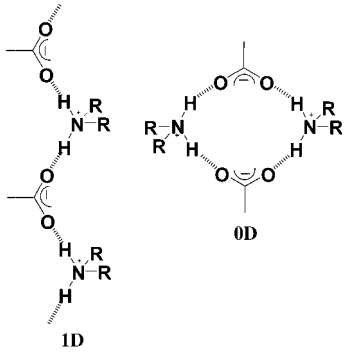

Scheme 2. Plausible 1D and 0D hydrogen-bonded motif in a secondary ammonium salt of monocarboxylic acid.

The fact that no halogen···halogen contacts can be seen in **1** (4-ClCIN) and **3** (4-BrCIN), and also that **5** (4-MeCIN) and **6** (CIN) displayed a similar hydrogen-bonded motif and packing, clearly indicate that the nature of substituents at the 4-position probably do not contribute much towards the overall packing in these gelator salts. However, it is worth

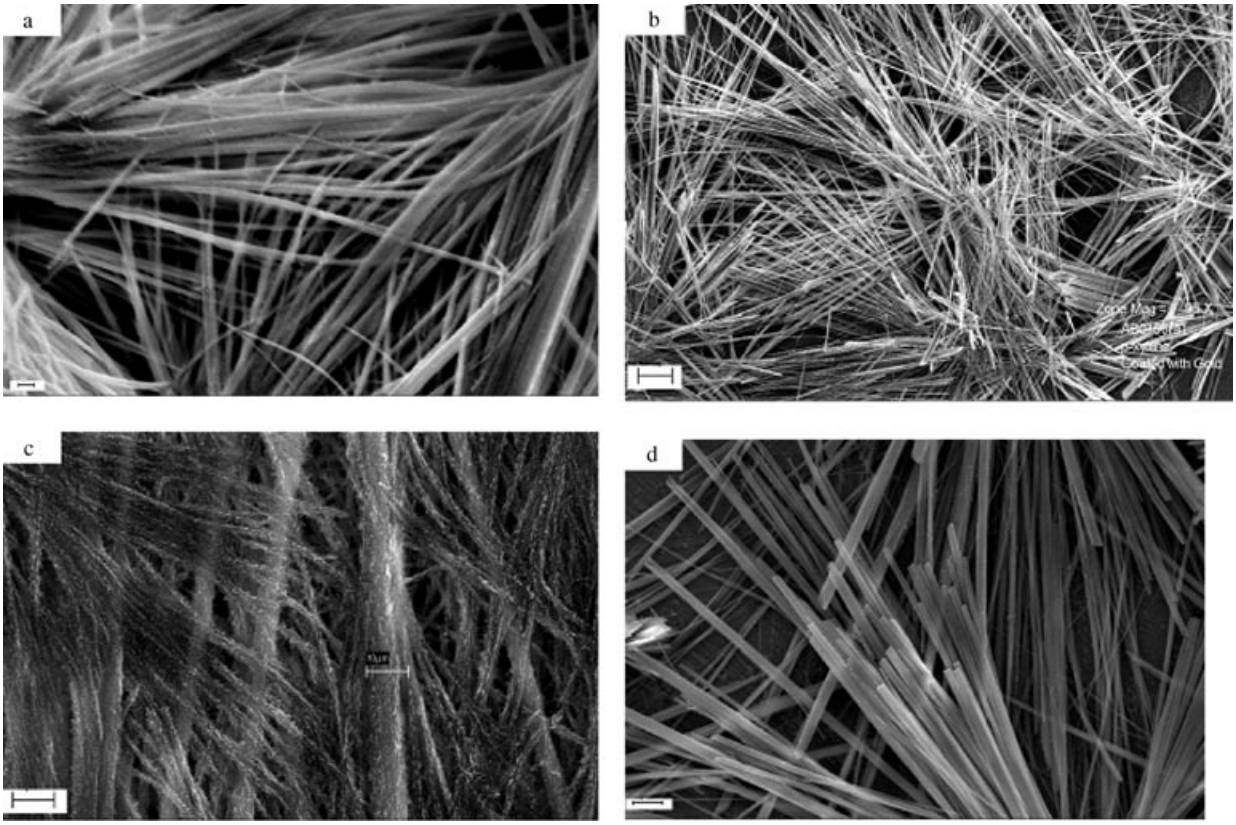

Figure 2. SEM of xerogel of a) **3** (4-BrCIN)/*p*-xylene (2.5 wt%), bar = 2 μm, b) **4** (3-BrCIN)/*p*-xylene (2.5 wt%), bar = 100 μm, c) **5** (4-MeCIN)/nitrobenzene (2.5 wt%), bar = 10 μm and d) **6** (CIN)/cyclohexane (1.3 wt%), bar = 10 μm.

Table 2. Crystallographic parameters for **1**, **3**, **5–6**, **8**, and **10–11**.

	1 (4-ClCIN)	**3** (4-BrCIN)	**5** (4-MeCIN)	**6** (CIN)	**8** (2-BrCIN)	**10** (2-MeCIN)	**11** (HyCIN)
empirical formula	$C_{21}H_{30}ClNO_2$	$C_{21}H_{30}BrNO_2$	$C_{22}H_{33}NO_2$	$C_{21}H_{31}NO_2$	$C_{21}H_{30}BrNO_2$	$C_{22}H_{33}NO_2$	$C_{21}H_{34}NO_{2.50}$
FW	363.91	408.37	343.49	329.47	408.37	343.49	340.49
crystal size [mm]	0.33 × 0.29 × 0.11	0.94 × 0.34 × 0.28	1.12 × 0.18 × 0.04	0.72 × 0.05 × 0.05	0.25 × 0.15 × 0.11	0.17 × 0.21 × 0.19	0.24 × 0.15 × 0.10
colour	colourless	colourless	colourless	colourless	colourless	colourless	colourless
crystal system	orthorhombic	monoclinic	orthorhombic	orthorhombic	monoclinic	monoclinic	monoclinic
space group	$P2_12_12_1$	$P2_1/c$	$P2_12_12_1$	$P2_12_12_1$	$P2_1/n$	$P2_1/a$	$C2/c$
a [Å]	5.797(5)	5.7497(4)	5.7903(9)	5.7000(11)	10.092(3)	9.105(9)	23.872(9)
b [Å]	17.282(15)	17.1165(12)	17.054(3)	16.640(3)	9.170(3)	21.000(9)	11.358(3)
c [Å]	20.532(18)	20.7991(15)	20.798(3)	20.762(4)	22.201(6)	10.650(6)	18.806(5)
α [°]	90.00	90.00	90.00	90.00	90.00	90.00	90.00
β [°]	90.00	93.4570(10)	90.00	90.00	96.73(3)	99.53(6)	127.31(3)
γ [°]	90.00	90.00	90.00	90.00	90.00	90.00	90.00
V [Å^{-3}]	2057(3)	2043.2(2)	2053.8(5)	1969.2(7)	2040.4(11)	2008(2)	4056(2)
Z	4	4	4	4	4	4	8
ρ_{calcd}	1.175	1.328	1.111	1.111	1.329	1.136	1.115
$F(000)$	784	856	752	720	856	752	1496
$\mu Mo_{K\alpha}$ [mm^{-1}]	0.199	2.025	0.070	0.070	2.028	0.071	0.072
T [K]	293(2)	293(2)	293(2)	293(2)	293(2)	293(2)	293(2)
obs refl. [$I > 2\sigma(I)$]	2386	3538	2337	2054	1513	1276	1582
parameters refined	226	346	224	217	298	334	294
goodness of fit	1.039	1.028	1.021	1.040	1.009	0.907	1.008
final $R1$ on observed data	0.0398	0.0527	0.0357	0.0485	0.0590	0.0569	0.0602
final $wR2$ on observe data	0.1036	0.1484	0.0905	0.1131	0.1462	0.1195	0.1581

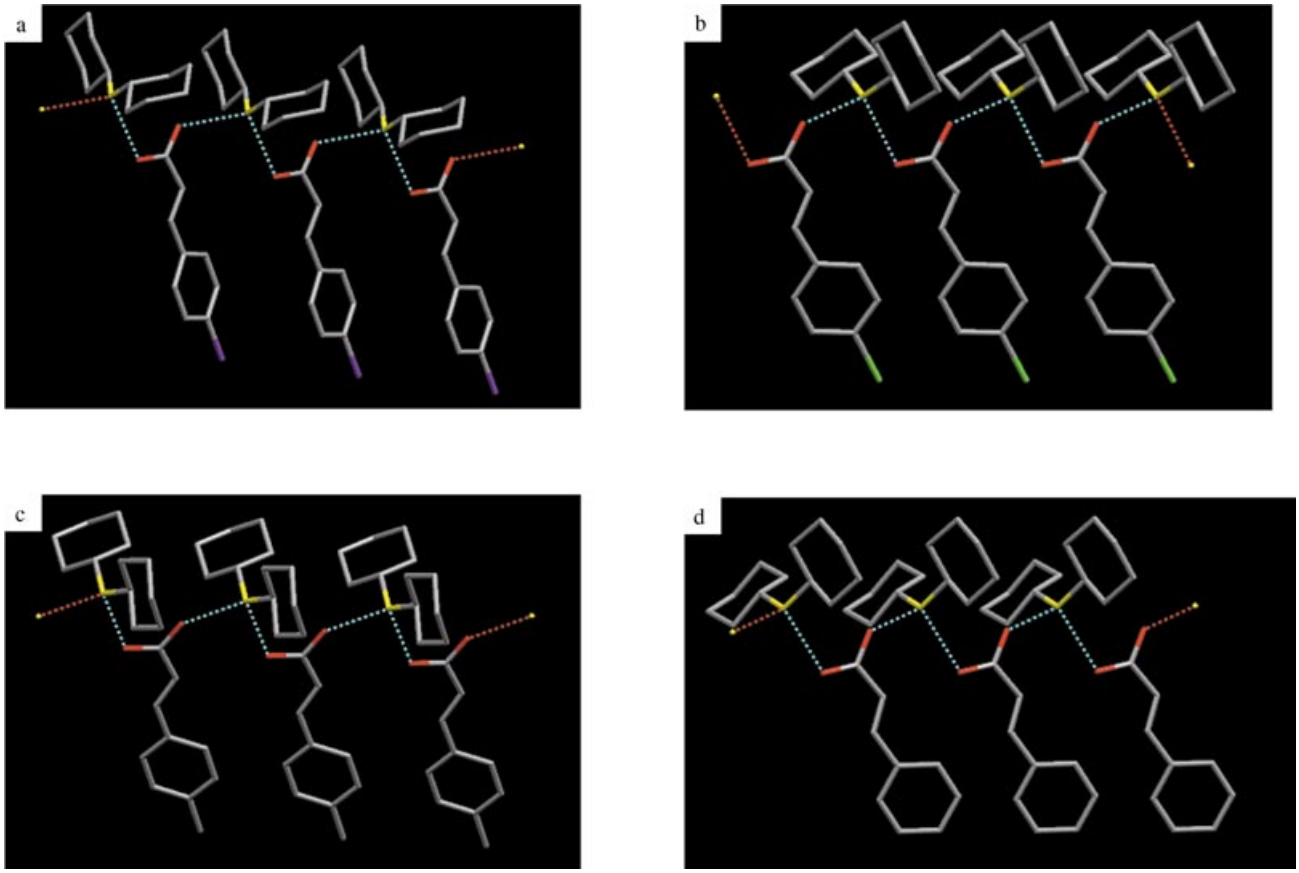

Figure 3. 1D hydrogen-bonded motif in the gelator crystal structures. a) in **1** (4-ClCIN), b) in **3** (4-BrCIN), c) in **5** (4-MeCIN), d) in **6** (CIN)].

noting that in all these structures, the 1D hydrogen-bonded motif is present and, therefore, it further supports the hypothesis that a 1D network promotes gelation. Despite our best efforts, we were not able to obtain crystals of **2** (3-ClCIN) and **4** (3-BrCIN) that were suitable for X-ray diffraction. After achieving this significant conclusion, we in-

vestigated the single-crystal structures of related non-gelator salts to establish the correlation between the molecular packing in the crystalline state and their non-gelation behaviour. Except **9** (3-MeCIN), all the non-gelator salts, namely, **8** (2-BrCIN), **10** (2-MeCIN), **11** (HyCIN) and all benzoate derivatives **12–18** were crystallised for single-crystal X-ray diffraction studies (Table 3). The crystal structure of **8** (2-BrCIN) is similar to that observed in **7** (2-ClCIN).[14]

In this structure (Figure 4), as in **7** (2-ClCIN), the expected 1D hydrogen-bonded motif arising from the ion pair is present. Significant Br···Br (3.538 Å) interactions[26] between the 1D chains make the overall network 2D, as in **7** (2-ClCIN) (Table 4). Thus, the observation that **8** (2-BrCIN) does not have any gelation ability is not a surprise because it agrees with the fact that a 2D network produces either a weak gel or does not promote gelation at all. It should be mentioned at this point that extended interdigitation of cinnamate groups is not seen in any of these compounds (gelators or non-gelators); however, non-extended head-to-tail arrangements of the cinnamate groups, which are less symmetrically oriented in gelators compared to that found in non-gelators, are also observed.

On the other hand, all the other non-gelators **10–18** show remarkable similarities in the hydrogen bonded motif. Thus, **10–18** show 0D cyclic hydrogen-bonded motif (Figure 5). The packing of the discrete 0D hydrogen-bonded assembly in these crystal structures appear to have been driven mainly by van der Waals interactions leading to a close pack (see the Supporting Information). It is interesting to note that a molecule of water (of crystallisation) is acting as a bridge between the 0D cyclic assemblies of the ion pair in **11** (HyCIN). However, it should be mentioned that significant Cl···Cl (3.489 Å) contacts are observed only in the 4-chlorobenzoate derivative **12**. Since, a 1D network is not achieved in these cases, these salts **10–18** do not have

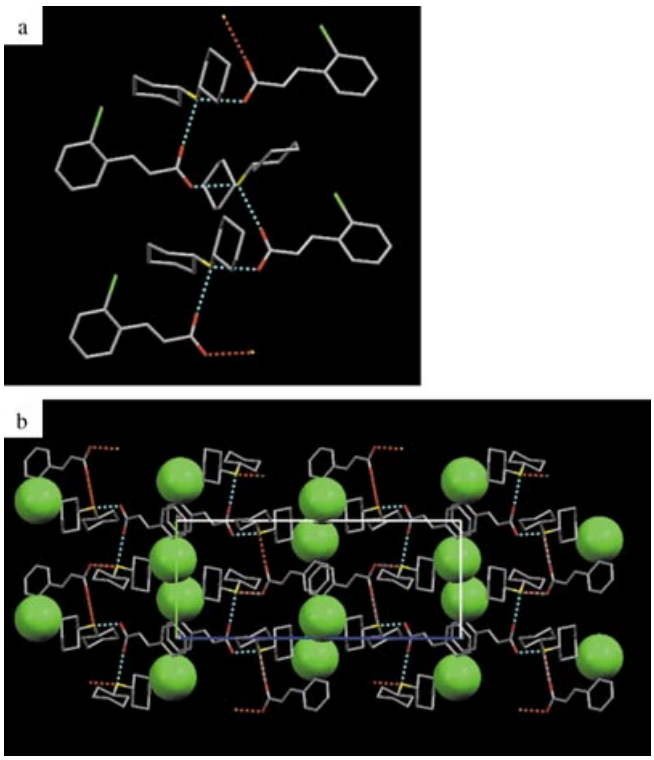

Figure 4. a) 1D hydrogen-bonded motif in **8** (2-BrCIN); b) overall molecular packing in the crystal lattice in **8** (2-BrCIN); Br atoms are represented by a space-filling model to emphasise their short contacts.

comply with prerequisite to become potential gelators and, therefore, they prefer the thermodynamically more stable crystalline state rather than the metastable gel state.

To address the second question, namely, how molecules pack in the fibres in the xerogel or gel state, we compared the powder diffraction patterns simulated from the corresponding single-crystal structures, experimental XRPD pat-

Table 3. Crystallographic parameters for **12–18**.

	12 (4-ClBNZ)	**13** (3-ClBNZ)	**14** (2-ClBNZ)	**15** (4-BrBNZ)	**16** (3-BrBNZ)	**17** (2-BrBNZ)	**18** (BNZ)
empirical formula	$C_{38}H_{56}Cl_2N_2O_4$	$C_{38}H_{56}Cl_2N_2O_4$	$C_{19}H_{28}ClNO_2$	$C_{19}H_{28}BrNO_2$	$C_{38}H_{56}Br_2N_2O_4$	$C_{19}H_{28}BrNO_2$	$C_{38}H_{58}N_2O_4$
FW	675.75	675.75	337.87	382.33	764.67	382.33	606.86
crystal size [mm]	1.07×0.29×0.13	0.18×0.21×0.19	0.19×0.16×0.20	1.27×0.71×0.37	0.89×0.35×0.21	0.23×0.16×0.11	0.18×0.20×0.19
colour	colourless	colourless	colourless	colourless	colourless	colourless	colourless
crystal system	monoclinic	triclinic	triclinic	triclinic	monoclinic	triclinic	monoclinic
space group	$P2_1/n$	$\bar{P}1$	$\bar{P}1$	$\bar{P}1$	$C2/c$	$\bar{P}1$	$P2_1/n$
a [Å]	11.3277(7)	9.528(3)	9.042(7)	9.105(3)	20.920(3)	9.208(8)	11.413(6)
b [Å]	21.2893(13)	11.660(5)	10.679(5)	10.558(3)	10.0821(12)	10.707(2)	20.165(9)
c [Å]	15.2943(9)	17.102(19)	10.687(4)	11.954(3)	36.005(4)	10.724(4)	15.438(12)
α [°]	90.00	91.38(6)	100.82(3)	110.104(4)	90.00	101.38(2)	90.00
β [°]	100.8980(10)	96.35(5)	113.98(4)	101.829(5)	92.945(2)	114.03(7)	102.94(6)
γ [°]	90.00	105.12(2)	90.00(5)	108.292(4)	90.00	90.19(6)	90.00
V [Å^{-3}]	3621.8(4)	1820(2)	922.7(9)	959.5(4)	7584.1(16)	942.5(9)	3463(4)
Z	4	2	2	2	8	2	4
ρ_{calcd}	1.239	1.233	1.216	1.323	1.339	1.347	1.164
$F(000)$	1456	728	364	400	3200	400	1328
$\mu Mo_{K\alpha}$ [mm^{-1}]	0.221	0.219	0.216	2.151	2.177	2.190	0.074
T [K]	293(2)	293(2)	293(2)	293(2)	293(2)	293(2)	293(2)
obs refl. [$I>2\sigma(I)$]	4279	3565	1575	3096	6121	1815	2270
parameters refined	415	639	279	320	423	320	400
goodness of fit	1.085	1.005	1.010	1.020	0.999	1.024	0.944
final $R1$ on observed data	0.0302	0.0653	0.0658	0.0455	0.0434	0.0417	0.1021
final $wR2$ on observe data	0.0833	0.1728	0.1967	0.1298	0.1079	0.0995	0.2528

Table 4. Hydrogen-bonding parameters for **1**, **3**, **5**, **6**, **8**, and **10–18**.

D–H···A	D–H [Å]	H···A [Å]	D···A [Å]	∢D-H···A [°]	Symmetry operation for A
1 (4-ClCIN)					
N(1)–H(1N2)···O(2)	0.90	1.83	2.731(3)	175.5	$-x+3/2, -y+1, z-1/2$
N(1)–H(1N1)···O(1)	0.90	1.85	2.751(3)	175.9	$-x+1/2, -y+1, z-1/2$
3 (4-BrCIN)					
N(1)–H(1N1)···O(1)	0.84(4)	1.89(4)	2.731(3)	177(3)	$-x+2, -y+1, -z+1$
N(1)–H(1N2)···O(2)	0.92(3)	1.82(3)	2.728(3)	172(3)	$-x+1, -y+1, -z+1$
5 (4-MeCIN)					
N(1)–H(1N2)···O(2)	0.90	1.80	2.702(2)	177.5	x, y, z
N(1)–H(1N1)···O(1)	0.90	1.83	2.731(2)	176.1	$x+1, y, z$
6 (CIN)					
N(1)–H(1N1)···O(2)	0.90	1.83	2.730(3)	174.3	x, y, z
N(1)–H(1N2)···O(1)	0.90	1.80	2.701(3)	174.0	$x-1, y, z$
8 (2-BrCIN)					
N(1)–H(1N2)···O(2)	0.84(5)	1.90(5)	2.735(6)	177(5)	$-x+1/2, y-1/2, -z+1/2$
N(1)–H(1N1)···O(1)	0.95(6)	1.75(6)	2.698(6)	179(5)	x, y, z
10 (2-MeCIN)					
N(1)–H(2N1)···O(2)	1.12(4)	1.62(4)	2.711(4)	163(3)	$-x+1, -y, -z+2$
N(1)–H(1N1)···O(1)	1.01(4)	1.73(4)	2.738(5)	172(3)	$x-1, y, z$
11 (HyCIN)					
N(1)–H(1N1)···O(2)	0.99(3)	1.75(3)	2.712(4)	163(3)	$-x+1/2, -y+3/2, -z+1$
O(1W)–H(1OW)···O(1)	0.95(4)	1.91(4)	2.847(4)	169(4)	x, y, z
N(1)–H(1N2)···O(1)	0.97(3)	1.77(4)	2.702(3)	159(3)	x, y, z
12 (4-ClBNZ)					
N(1)–H(1N2)···O(2)	0.90	1.86	2.7480(15)	168.6	$-x+1/2, y-1/2, -z+3/2$
N(1)–H(1N1)···O(2′)	0.90	1.82	2.7123(15)	169.4	$-x+3/2, y-1/2, -z+3/2$
N(2)–H(2N1)···O(1)	0.90	1.83	2.7246(15)	172.1	$x+1, y, z$
N(2)–H(2N2)···O(1′)	0.90	1.86	2.7420(15)	167.4	x, y, z
13 (3-ClBNZ)					
N(1)–H(1N1)···O(2′)	0.93(3)	1.80(4)	2.725(5)	168(3)	x,y,z
N(1)–H(1N2)···O(1′)	0.83(3)	1.87(4)	2.689(4)	169(3)	$-x+1, -y, -z+1$
N(2)–H(2N1)···O(2)	0.78(3)	1.94(3)	2.712(4)	170(3)	$-x, -y+1, -z+1$
N(2)–H(2N2)···O(1)	0.97(4)	1.74(4)	2.700(5)	173(3)	$x, y, z-1$
14 (2-ClBNZ)					
N(1)–H(1N1)···O(1)	1.01(4)	1.73(4)	2.729(5)	168(3)	$-x+1, -y, -z+2$
N(1)–H(2N1)···O(2)	0.86(4)	1.86(4)	2.701(5)	166(3)	$x, y-1, z$
15 (4-BrBNZ)					
N(1)–H(1N1)···O(2)	0.87(3)	1.86(3)	2.723(3)	174(3)	x, y, z
N(1)–H(1N2)···O(1)	0.87(3)	1.86(3)	2.716(3)	169(3)	$-x+1, -y+1, -z+1$
16 (3-BrBNZ)					
N(1′)–H(1N3)···O(2′)	0.90	1.85	2.715(2)	161.6	x, y, z
N(1′)–H(1N4)···O(2)	0.90	1.87	2.755(2)	168.9	x, y, z
N(1)–H(1N2)···O(1′)	0.90	1.83	2.701(2)	163.9	$-x+1/2, -y+1/2, -z+1$
N(1)–H(1N1)···O(1)	0.90	1.80	2.688(2)	169.3	$-x+1/2, -y+1/2, -z+1$
17 (2-BrBNZ)					
N(1)–H(1N1)···O(1)	1.06(4)	1.72(4)	2.751(5)	162(3)	$-x, -y+2, -z$
N(1)–H(1N2)···O(2)	0.90(4)	1.81(4)	2.698(4)	166(3)	$x, y+1, z$
18 (BNZ)					
N(1)–H(1N1)···O(1)	1.00(4)	1.72(4)	2.697(4)	164(3)	$-x-1/2, y+1/2, -z+3/2$
N(1)–H(1N2)···O(2′)	0.86(4)	1.90(4)	2.736(4)	164(4)	$x, y, z+1$
N(2)–H(2N1)···O(1′)	0.90	1.84	2.718(4)	165.9	$x+1,y, z$
N(2)–H(2N2)···O(2)	0.90	1.83	2.714(4)	167.2	$-x+1/2, y+1/2, -z+1/2$

terns of the bulk solids and xerogels of **1** (4-ClCIN), **3** (4-BrCIN), **5** (4-MeCIN) and **6** (CIN). A close examination of Figure 6 reveals that, in all these cases, the corresponding major peak positions match those in the simulated patterns, XRPD of bulk solids and xerogels. However, the relative intensities of a few peaks are affected, and this could be caused by preferred orientations of crystallites.[18] Therefore, it may be concluded that the respective patterns in these gelators are nearly identical, which indicates that the molecular packing of the gelator molecules obtained from single-crystal X-ray diffraction truly represents the molecular packing in the bulk solids and xerogel. Considering the fact that a solid–solid morphological change of the fibres of the gel (during the transformation from gel to xerogel) can be induced either by solvent removal (while forming xerogel) or by nucleation events initiated by the small amount of gelator that might be present in the solution in the bulk liquid in gelled state, there is no certainty that the molecular packing in the fibre of a xerogel truly represents that in the gelled state. However, attempts to record the XRPD in the gel state for all of these gelators have failed, presumably as a result of strong scattering from the solvent molecules. Since the morph responsible for gel formation might not be the thermodynamically most stable one and therefore, such a phase transformation is quite possible during removal of the solvent during xerogel formation. There is no certainty that

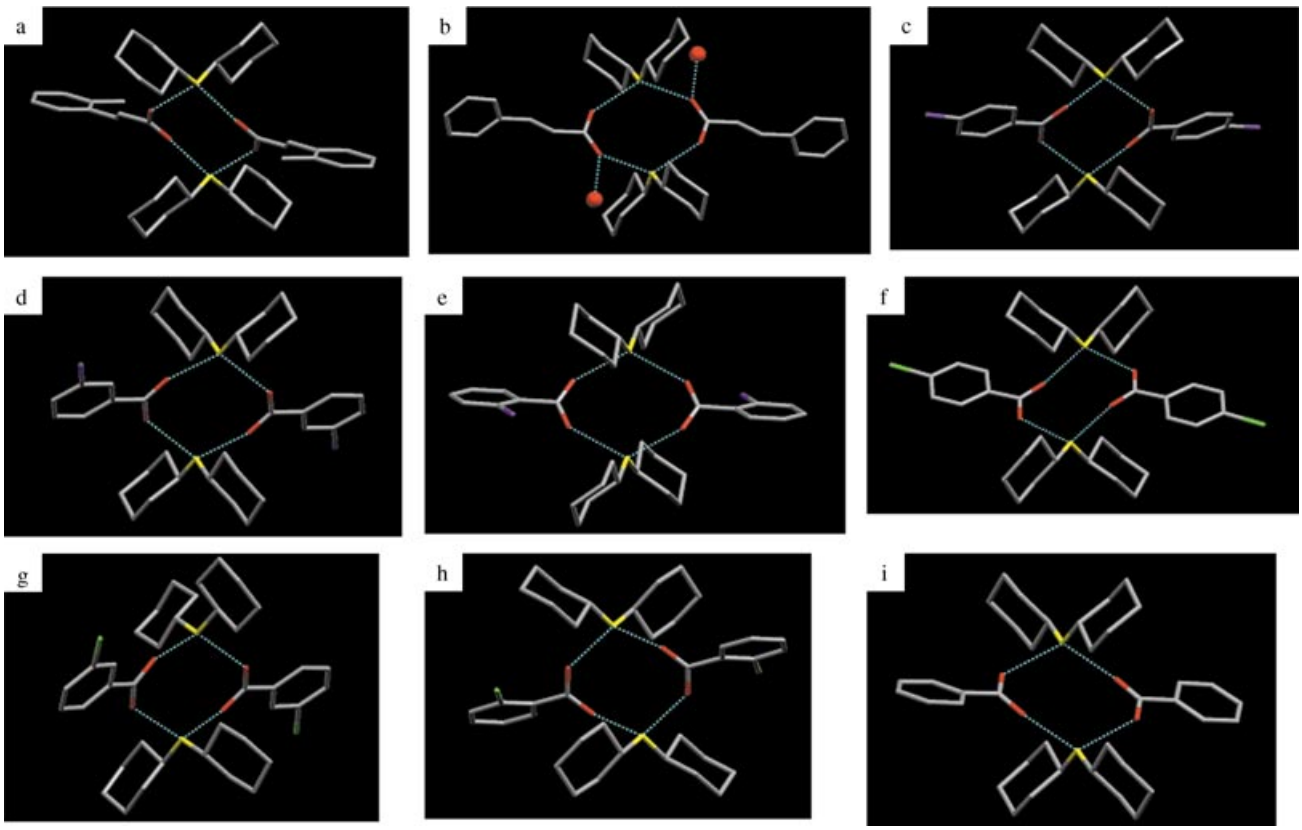

Figure 5. 0D hydrogen-bonded motif in the non-gelators. a) in **10** (2-MeCIN), b) in **11** (HyCIN), c) in **12** (4-ClBNZ), d) in **13** (3-ClBNZ), e) in **14** (2-ClBNZ), f) in 15 (4-BrBNZ), g) in **16** (3-BrBNZ), h) in **17** (2-BrBNZ), i) in **18** (BNZ).

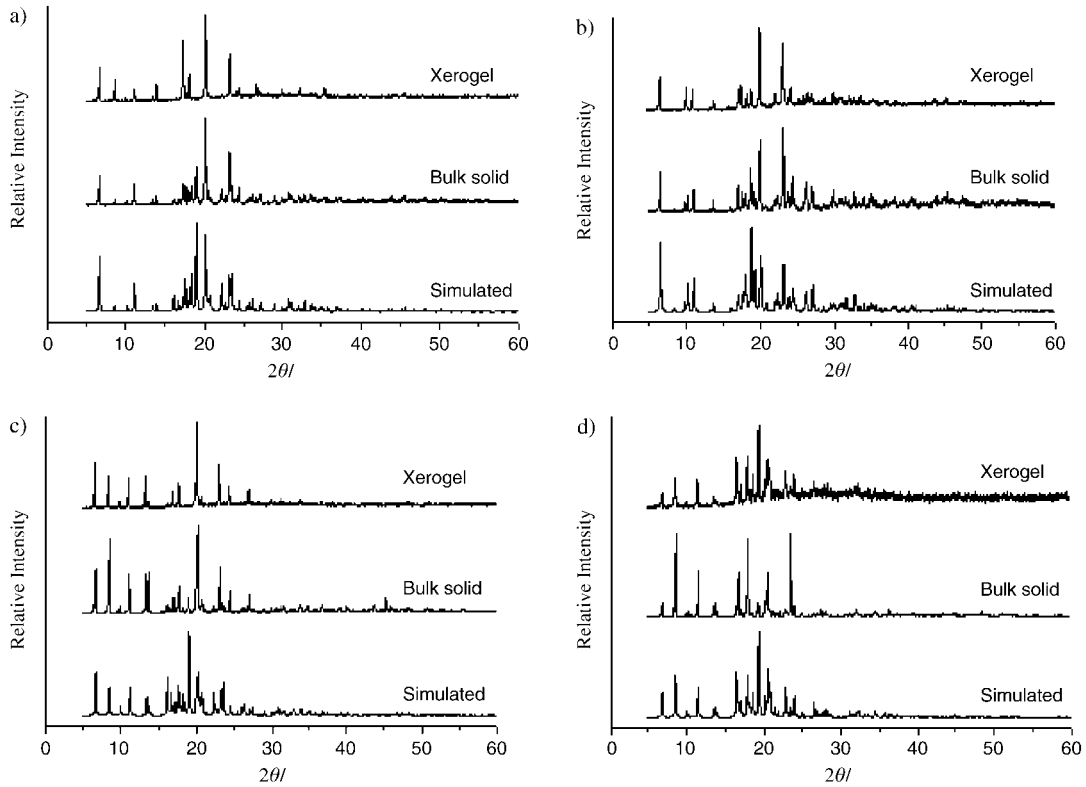

Figure 6. XRPD patterns ($Cu_{K\alpha}$ radiation, $\lambda = 1.5418$ Å) under various conditions for the gelators. a) **1** (4-ClCIN), xerogel from nitrobenzene (1.0 wt%), b) **3** (4-BrCIN), xerogel from *n*-heptane (1.0 wt%), c) **5** (4-MeCIN), xerogel from *m*-xylene (1.0 wt%), d) **6** (CIN), xerogel from cyclohexane (1.0 wt%).

such a change does occur during xerogel formation, but there is no evidence that it does not. Therefore, the molecular packing of the fibres in the xerogel of these gelators **1** (4-ClCIN), **3** (4-BrCIN), **5** (4-MeCIN) and **6** (CIN) can be considered similar to that observed in their respective thermodynamically more stable crystalline state revealed by single-crystal X-ray diffraction studies. However, no comments on the molecular packing in the gelled state of these gelators can be made.

As demonstrated in these studies as well as in earlier reports,[16] the prerequisite of gel formation is the one-dimensional alignment of gelator molecules supported by hydrogen bonding. Furthermore, hydrogen bonding and π-stacking-induced supramolecular assembly in gelators are also reported.[19] Taking into consideration the fact that the cinnamic acid moiety contains a π-conjugated system whose importance in the gelation process is also apparent because none of the salts devoid of a conjugated olefinic double bond (**11**–**18**) show any gelation ability, we decided to examine the role of π–π interactions between the cinnamate moieties that might contribute towards the formation of organogels.

To examine the role of π–π interactions in these cinnamate salts, we employed ab initio quantum chemical calculations at the HF/3-21G* level of theory.[20] The relative orientation of cinnamates obtained in the crystal structures for some of these organic salts is compared to the calculated results. To facilitate the calculations, substituted ammonium cinnamates were considered as models. The orientation of two interacting cinnamates is considered to be in the α form (head-to-tail) because the cinnamates are in the α form in the present crystal structures. Chloro and methyl groups are considered as substituents in the calculations. The results of 2-, 3-, 4-chloro- and the corresponding methylcinnamates are shown in Figure 7. The calculated gas-phase structures, optimised at the HF/3-21G* level, for 2-, 3- and 4-chlorocinnamates show that the relative orientation of the cinnamates are distorted. In the case of 2-chlorocinnamate, the olefinic π units do not lie in the plane of the phenyl ring and hence such a distortion does not allow the cinnamates to achieve π–π stacking (Figure 7a). However, the structure obtained from X-ray crystallographic analysis shows that the 2-chlorocinnamate molecules in **7** (2-ClCIN)[14] are stacked for π–π interactions (Figure 7b). An examination of the calculated geometries for 3- and 4-chlorocinnamates indicates that the olefinic π units have less deviation from the phenyl ring in comparison to the calculated geometry of 2-chlorocinnamate. However, they are also not packed for π–π interactions (Figure 7c, Figure 7d). In particular, offset geometries are predicted in these two cases.

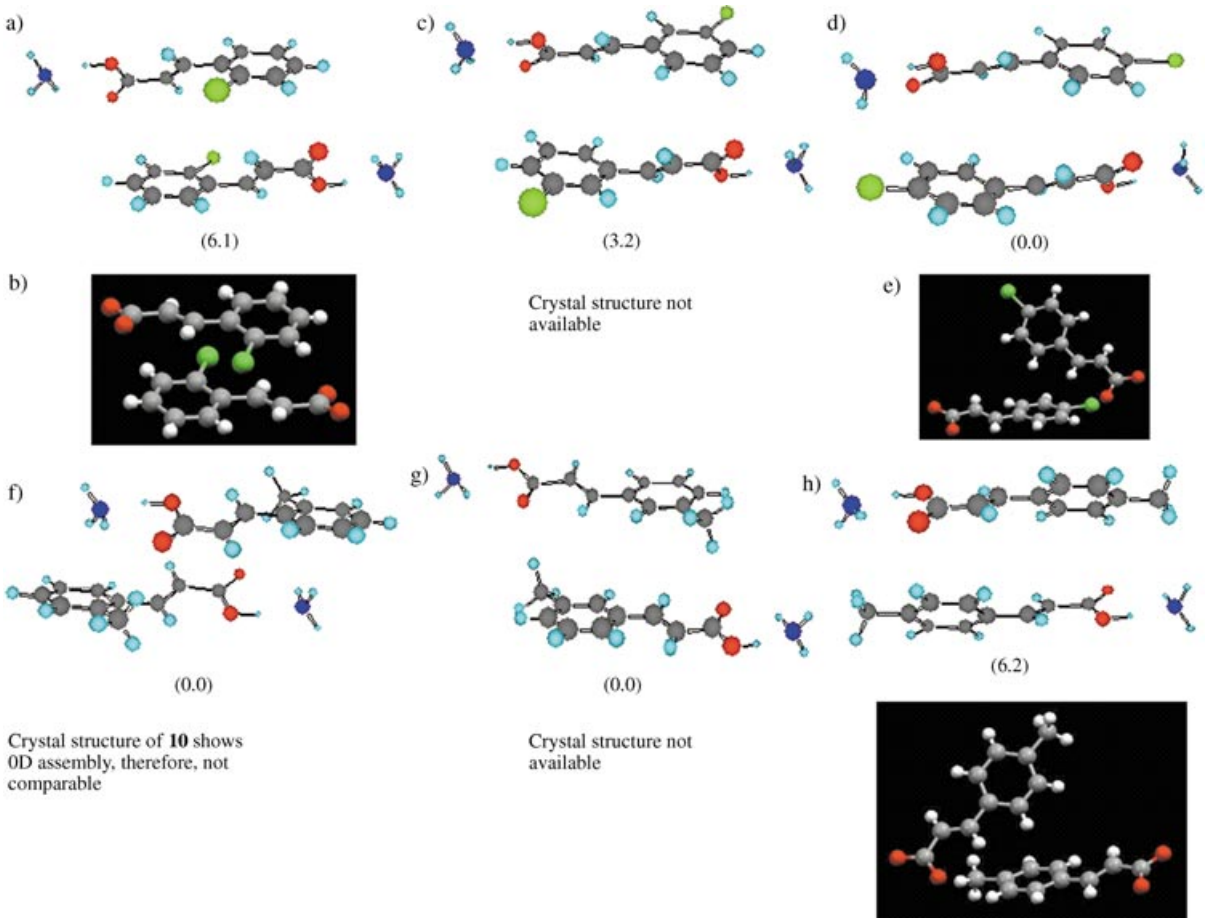

Figure 7. Optimised geometry of a) ammonium 2-chlorocinnamate, c) ammonium 3-chlorocinnamate, d) ammonium 4-chlorocinnamate, f) ammonium 2-methylcinnamate, g) ammonium 3-methylcinnamate, h) ammonium 4-methylcinnamate; relative orientation of the anions in the crystal structure of b) **7** (2-ClCIN), e) **1** (4-ClCIN), and i) **5** (4-MeCIN); values in the parenthesis represent the relative energies in kcal mol^{-1}.

In the crystal structure of **1** (4-ClCIN) (Figure 7e), the relative orientation of the anions is found to be more distorted than that observed in the calculated structure (Figure 7d). The calculated energies predict that the 4-chlorocinnamate is the most stable, while the 2-chlorocinnamate is the least stable of the series (Figure 7). The energy differences in these cases arise presumably as a result of other nonbonded and steric interactions. However, it is clear from the calculations that none of these chlorocinnamates exhibits a geometry that is conducive for effective π–π stacking interactions. The fact that 2-chlorocinnamate **7** (2-ClCIN) is a non-gelator and 4-chlorocinnamate **1** (4-ClCIN) is an efficient gelator clearly suggests that π–π stacking interactions are not the driving force for gelation process in these cases.

The calculated results for methylcinnamate show that the 2-methylcinnamate converges with the slipped geometry (Figure 7f). However, 3- and 4-methylcinnamates have been predicted to have offset geometry (Figure 7g, Figure 7h, respectively). The crystal structure obtained for **5** (4-MeCIN) shows that the anion moieties are almost perpendicular to each other (Figure 7i). Therefore, such an arrangement of cinnamate moieties does not achieve the π–π interactions in this case. The calculated energies are comparable for 2- and 3-methylcinnamates, whereas 4-methylcinnamate is predicted to be the least stable of the series (Figure 7). Structures predicted from the calculations do not show geometry conducive to π–π stacking interactions. The crystal structure of **5** (4-MeCIN), which is a gelator, also displays no π–π interactions, which indicates that π–π stacking interactions are not important for gelation in these cases.

Overall, the combined analysis of calculated and crystal structures suggest that the formation of an organogel is not governed by the π–π interactions in this class of gelators.

Conclusion

A novel class of LMOGs based on various cinnamate salts has been discovered. Their facile preparation and efficient gelation ability, including selective gelation of oil from a oil/water mixture, make this novel class of LMOGs attractive. Successful determination of the single-crystal structures of most of the gelators, which are not so common in the related literature, and that of related non-gelators allowed us to correlate the molecular packing of the gelators and non-gelators in their crystalline state and their corresponding gelling/non-gelling ability. All the gelators that could be crystallised for X-ray diffraction show 1D network of ion pairs, without any exceptions. On the other hand, all the non-gelators exhibit discrete 0D assemblies of the ion pair, except 2-chlorocinnamate salt **7** (2-ClCIN) and the corresponding 2-Br derivative **8** (2-BrCIN). In these structures, significant halogen···halogen interactions have prompted the 1D hydrogen-bonded ion pair to assemble in a 2D fashion. Therefore, the prerequisite to grow the gel fibrils in one direction seems to originate from the hydrogen-bonded 1D network involving the ion pair in these gelators. Although the molecular self-assembly of the fibres in the gelled state cannot be established, the presence of a 1D hydrogen-bonded network of the ion pair in the fibres of the xerogels is quite evident from the simulated powder diffraction patterns and XRPDs of the xerogel comparison. It is not mandatory that the crystal structure of the fibres in the xerogel must be identical to that in the gelled state because morphological transformation may occur during xerogel formation. However, it may be reasonable to assume that the main driving force of the 1D growth of the gel fibres is mainly governed by the 1D hydrogen-bonded network of ion pairs, although the overall crystal structure of the gel fibrils might be different from that in the xerogel. π–π stacking interactions do not seem to be important for the gelation process in this class of gelators, as observed by computed and crystal structure analyses. We believe that the present study represents one of the most explicit cases wherein the molecular packing of the gelator and non-gelator molecules in their crystalline state can be directly correlated to their gelling/non-gelling ability.

Experimental Section

Materials and physical measurements: All chemicals (Aldrich) and the solvents used for gelation (A. R. grade, S. D. Fine Chemicals, India) are used without further purification. All the oils were purchased locally. Microanalyses were performed on a Perkin Elmer elemental analyzer 2400, Series II. FT-IR and NMR spectra were recorded on a Perkin-Elmer Spectrum GX and 200 MHz Bruker Avance DPX_{200} spectrometers, respectively. The X-ray powder patterns were recorded on a XPERT Philips ($Cu_{K\alpha}$ radiation) diffractometer. Scanning Electron Microscopy (SEM) was performed on a LEO 1430 VP.

Syntheses

Salt 3 (4-BrCIN): A solution 4-bromocinnamic acid (1.0 mmol) in hot nitrobenzene was prepared with the aid of few drops of MeOH. To this solution, was slowly added dicyclohexylamine (1.0 mmol), and the reaction mixture was kept at room temperature for a few hours to gel the whole reaction mixture. Acetonitrile was then added to the gel to destroy the gel network and to precipitate white **3**, which was then isolated by filtration (near quantitative yield) and used for gelation and other studies.

Salts 4–18: The corresponding acid (1.0 mmol) was dissolved in MeOH by sonication. Dicyclohexylamine (1.0 mmol) was added slowly to the methanolic solution of the acid at room temperature. The reaction mixture was then allowed to evaporate to dryness at room temperature. The resulting salts were obtained as white precipitates (near quantitative yield), and were used for gelation and other studies.

Analytical data:

3 (4-BrCIN): M.p. 190–191 °C; ^{1}H NMR (200 MHz, CD_3OD): δ = 7.29–7.49 (m, 5H), 6.47–6.55 (m, 1H), 3.16 (m, 2H), 1.70–2.04 (m, 10H), 1.28–1.42 ppm (m, 10H); elemental analysis calcd (%) for $C_{21}H_{30}BrNO_2$: C 61.71, H 7.35, N 3.43; found: C 61.54, H 7.64, N 3.62.

4 (3-BrCIN): M.p. 146–147 °C; ^{1}H NMR (200 MHz, CD_3OD): δ = 7.23–7.69 (m, 5H), 6.47–6.55 (d, 1H), 3.13–3.22(m, 2H), 1.70–2.08 (m, 10H), 1.22–1.49 ppm (m, 10H); elemental analysis calcd (%) for $C_{21}H_{30}BrNO_2$: C 61.71, H 7.35, N 3.43; found: C 61.64, H 6.67, N 3.31.

5 (4-MeCIN): M.p. 206 °C; ^{1}H NMR (200 MHz, CD_3OD): δ = = 7.38–7.49 (m, 3H), 7.14–7.32 (m, 2H), 6.41–6.49 (d, 1H), 3.10–3.15 (m, 2H), 1.69–2.06 (m, 10H), 0.97–1.42 (m, 10H), 2.33 ppm (s, 3H); elemental analysis calcd (%) for $C_{22}H_{33}NO_2$: C 76.92, H 9.68, N 4.08; found: C 77.05, H 9.78, N 4.11.

6 (CIN): M.p. 182 °C; ^{1}H NMR (200 MHz, CD_3OD): δ = = 7.34–7.52 (m, 6H), 6.49–6.57 (d, 1H), 3.16 (m, 2H), 1.68–2.07 (m, 10H), 1.32–1.36 ppm (m, 10H); elemental analysis calcd (%) for $C_{21}H_{31}NO_2$: C 76.55, H 9.48, N 4.25; found: C 76.71, H 9.65, N 4.30.

8 (2-BrCIN): M.p. 154–156 °C; ^{1}H NMR (200 MHz, CD_3OD): δ = 7.17–7.81(m, 5H), 6.43–6.51 (d, 1H), 3.17(m, 2H), 1.69–2.15 (m, 10H), 1.22–

1.48 ppm (m, 10H); elemental analysis calcd (%) for $C_{21}H_{30}BrNO_2$: C 61.71, H 7.35, N 3.43; found: C 61.87, H 6.90, N 3.33.

9 (3-MeCIN): M.p. 148 °C; ^{1}H NMR (200 MHz, CD_3OD): δ = 7.10–7.50 (m, 5H), 6.44–6.52 (d, 1H), 3.12–3.15 (m, 2H), 1.68–2.07 (m, 10H), 1.16–1.41 (m, 10H), 2.34 ppm (s, 3H); elemental analysis calcd (%) for $C_{22}H_{33}NO_2$: C 76.92, H 9.68, N 4.08; found: C 76.93, H 9.45, N 4.16.

10 (2-MeCIN): M.p.150 °C; ^{1}H NMR (200 MHz,CD_3OD): δ = 7.68–7.76 (d, 1H), 7.51–7.53 (m, 1H), 7.17 (m, 3H), 6.36–6.43 (d, 1H), 3.15 (m, 2H), 1.68–2.06 (m, 10H), 1.02–1.48 (m, 10H), 2.40 ppm (s, 3H); elemental analysis calcd (%) for $C_{22}H_{33}NO_2$: C 76.92, H 9.68, N 4.08; found: C 77.01, H 9.55, N 4.09.

11 (HyCIN): M.p.146–148 °C; ^{1}H NMR (200 MHz, CD_3OD): δ = 7.11–7.23 (m, 5H), 3.10–3.14 (m, 2H), 2.85–2.94 (t, 2H), 2.39- 2.47 (t, 2H), 1.68–2.05 (m, 10H), 1.22–1.46 ppm (m, 10H); elemental analysis calcd (%) for $C_{21}H_{33}O_2$ .2 H_2O: C 68.63, H 10.15, N 4.10; found: C 69.00, H 10.59, N 3.81.

12 (4-ClBNZ): M.p. 182 °C; ^{1}H NMR (200 MHz, CD_3OD): δ = 7.88–7.92 (m, 2H) 7.32–7.36 (m, 2H), 3.13–3.19(m, 2H), 1.68–2.07 (m, 10H), 1.21–1.42 ppm (m, 10H); elemental analysis calcd (%) for $C_{19}H_{28}ClNO_2$: C 67.54, H 8.35, N 4.15; found: C 67.33, H 8.47, N 4.14.

13 (3-ClBNZ): M.p. 178 °C; ^{1}H NMR (200 MHz, CD_3OD): δ = 7.82–7.91 (m, 2H), 7.28–7.41 (m, 2H), 3.17 (m, 2H), 1.69–2.08 (m, 10H), 1.16–1.48 ppm (m, 10H); elemental analysis calcd (%) for $C_{19}H_{28}ClNO_2$: C 67.54, H 8.35, N 4.15; found: C 67.41, H 8.67, N 4.19.

14 (2-ClBNZ): M.p. 180–182 °C; ^{1}HNMR (200 MHz,CD_3OD): δ = 7.21–7.42 (m, 4H), 3.17 (m, 2H), 1.69–2.07 (m, 10H), 1.16–1.48 ppm (m, 10H); elemental analysis calcd (%) for $C_{19}H_{28}ClNO_2$: C 67.54, H 8.35, N 4.15; found: C 67.41, H 8.46, N 4.07.

15 (4-BrBNZ): M.p. 178–180 °C; ^{1}H NMR (200 MHz, CD_3OD): δ = 7.74–7.91 (d, 2H), 7.40–7.57 (d, 2H), 2.87–3.26 (m, 2H), 1.59–2.18 (m, 10H), 1.05–1.51 ppm (m, 10H); elemental analysis calcd (%) for $C_{19}H_{28}BrNO_2$: C 59.69, H 7.38, N 3.66; found: C 59.47, H 7.49, N 3.75.

16 (3-BrBNZ): M.p.186–188 °C; ^{1}H NMR (200 MHz, CD_3OD): δ = 8.078 (s, 1H), 7.86–7.90 (d, 1H), 7.52–7.56(d, 1H), 7.23–7.30 (t, 1H), 3.14–3.23 (m, 2H), 1.69–2.07 (m, 10H), 1.16–1.58 ppm (m, 10H); elemental analysis calcd (%) for $C_{19}H_{28}BrNO_2$: C 59.69, H 7.38, N 3.66; found: C 59.67, H 7.29, N 3.50.

17 (2-BrBNZ): M.p. 200–202 °C; ^{1}H NMR (200 MHz, CD_3OD): δ = 7.49–7.53 (d, 1H), 7.25–7.40 (m, 2H), 7.10–7.18 (t, 1H), 3.11–3.24 (m, 2H), 1.69–2.07 (m, 10H), 1.16–1.48 ppm (m, 10H); elemental analysis calcd (%) for $C_{19}H_{28}BrNO_2$: C 59.69, H 7.38, N 3.66; found: C 59.50, H 7.02, N 3.62.

18 (BNZ): M.p. 194 °C; ^{1}H NMR (200 MHz, CD_3OD): δ = 7.92–7.95 (m, 2H), 7.34–7.37 (m, 3H), 3.13–3.15 (m, 2H), 1.68–2.06 (m, 10H), 1.15–1.47 ppm (m, 10H); elemental analysis calcd (%) for $C_{19}H_{29}NO_2$: C 75.21, H 9.63, N 4.62; found: C 75.05, H 9.60, N 4.92.

Gelation experiments: In a typical experiment, the gelator (10 mg) was dissolved in a suitable solvent (1 mL) by heating in the presence of a few drops of MeOH. The mixture was left to cool to room temperature. After a few hours, when the solution appeared as solid-like material, the container was inverted. The material was considered to be a gel if it did not deform. If it flowed slightly, it was considered to be a viscous liquid.

Gel-to-sol dissociation temperature (T_{gel}) measurement: T_{gel} was measured by the following method. The gel was (1.0 mL) prepared in a test tube (15 mm diameter). A locally made glass ball weighing 0.195 g was placed on the gel surface. The test tube was then heated in an oil bath. The temperature (T_{gel}) was noted when the ball fell to the bottom of the test tube.

SEM measurement: A hot solution of gelator (50 μL) was placed on the SEM sample holder and allowed to form a gel, which was then dried in a vacuum. The dried gel was then subjected to gold sputtering by a Polaron SC7620 sputter coater. The gold-coated sample was used for direct viewing with a LEO 1430 VP SEM instrument.

Single-crystal X-ray diffraction: X-ray quality single crystals were grown under slow evaporative conditions at room temperature to give crystals of **1**, **3**, **5** from MeOH/water, **6** from *p*-xylene/MeOH, **8** from ethyl acetate, **10** from *n*-heptane/MeOH, **11** from *n*-octane, **12**, **15**, and **18** from MeOH, **13** and **14** from isobutanol/MeOH, and **16** and **17** from ethanol. Diffraction data for **1**, **3**, **5**, **6**, **12**, **15**, **16** were collected with $Mo_{K\alpha}$ (λ = 0.7107 Å) radiation on a SMART APEX diffractometer equipped with a CCD area detector. Data for other crystals were collected with $Mo_{K\alpha}$ (λ = 0.7107 Å) radiation on a CAD-4 diffractometer. Data collection, data reduction, structure solution/refinement were carried out with the software package of SMART APEX for **1**, **3**, **5**, **6**, **12**, **15**, and **16**, whereas the corresponding calculations were performed for the data collected on CAD-4 with CAD4-PC,[21] NRCVAX,[22] SHELX97.[23] Graphics were generated with PLATON[24] and MERCURY 1.1.1.[25]

All structures were solved by direct methods and refined in a routine manner. In all cases, non-hydrogen atoms were treated anisotropically. Whenever possible, the hydrogen atoms were located on a difference Fourier map and refined. In other cases, the hydrogen atoms were geometrically fixed. The crystallographic parameters are listed in Tables 2 and 3. The hydrogen-bonding parameters are given in Table 4.

CCDC-230578–CCDC-230591 contain the supplementary crystallographic data for this paper. These data can be obtained free of charge via www.ccdc.cam.ac.uk/conts/retrieving.html (or from the Cambridge Crystallographic Data Centre, 12 Union Road, Cambridge CB21EZ, UK; fax: (+44) 1223-336033; or deposit@ccdc.cam.uk).

Acknowledgments

Ministry of Environment and Forests, New Delhi is acknowledged for financial support. We thank Dr. P. K. Ghosh for his support.

[1] a) P. Terech, R. G. Weiss, *Chem. Rev.* **1997**, *97*, 3133–3160; b) J. Prost, F. Rondelez, *Nature* **1991**, *350*, 11 (supplement); c) J. van Esch, B. L. Feringa, *Angew. Chem.* **2000**, *112*, 2351–2354; *Angew. Chem. Int. Ed.* **2000**, *39*, 2263–2266;d) D. J. Abdallah, R. G. Weiss, *Adv. Mater.* **2000**, *12*, 1237–1247; e) O. Grownwald, S. Shinkai, *Chem. Eur. J.* **2001**, *7*, 4328–4334; f) J. C. Tiller, *Angew. Chem.* **2003**, *115*, 3180–3183; *Angew. Chem. Int. Ed.* **2003**, *42*, 3072–3075; g) F. M. Menger, A. V. Peresypkin, *J. Am. Chem. Soc.* **2003**, *125*, 5340–5345; h) F. M. Menger, Y. Yamasaki, K. K. Catlin, T. Nishimi, *Angew. Chem.* **1995**, *107*, 616–617; *Angew. Chem. Int. Ed. Engl.* **1995**, *34*, 585–586; i) M. Kölbel, F. M. Menger, *Chem. Commun.* **2001**, 275–276; j) A. Heeres, C. van der Pol, M. Stuart, A. Friggeri, B. L. Feringa, J. van Esch, *J. Am. Chem. Soc.* **2003**, *125*, 14252–14253; k) D. J. Abdallah, R. G. Weiss, *Chem. Mater.* **2000**, *12*, 406–413; l) C. Wang, A. Robertson, R. G. Weiss, *Langmuir* **2003**, *19*, 1036–1046;m) B. A. Simmons, C. E. Taylor, F. A. Landis, V. T. John, G. L. McPherson, D. K. Schwartz, R. Moore, *J. Am. Chem. Soc.* **2001**, *123*, 2414–2421;n) O. Gronwald, S. Shinkai, *Chem. Eur. J.* **2001**, *7*, 4329–4334; o) R. Wang, C. Geiger, L. Chen, B. Swanson, D. G. Whitten, *J. Am. Chem. Soc.* **2000**, *122*, 2399–2400.

[2] Steroid-based gelators: a) Y. Lin, B. Kachar, R. G. Weiss, *J. Am. Chem. Soc.* **1989**, *111*, 5542–5551; b) U. Maitra, S. Mukhopadhyay, A. Sarkar, P. Rao, S. S. Indi, *Angew. Chem.* **2001**, *113*, 2341–2343; *Angew. Chem. Int. Ed.* **2001**, *40*, 2281–2283; c) S. Kawano, N. Fujita, K. J. C. van Bommel, S. Shinkai, *Chem. Lett.* **2003**, *32*, 12–13; d) M. Numata, S. Shinkai, *Chem. Lett.* **2003**, *32*, 308–309.

[3] Carbohydrate-based gelators: a) K. Inoue, Y. Ono, Y. Kanekiyo, S. Kiyonaka, I. Hamachi, S. Shinkai, *Chem. Lett.* **1999**, 225–226; b) S. Bhattacharya, S. N. Ghanashyam Acharya, *Chem. Mater.* **1999**, *11*, 3504–3511; c) S. Yamasaki, H. Tsutsumi, *Bull. Chem. Soc. Jpn.* **1996**, *69*, 561–564; d) A. Friggeri, O. Gronwald, K. J. C. van Bommel, S. Shinkai, D. N. Reinhoudt, *J. Am. Chem. Soc.* **2002**, *124*, 10754–10758; e) R. J. H. Hafkamp, B. P. A. Kokke, I. M. Danke, H. P. M. Geurts, A. E. Rowan, M. C. Feitersa, R. J. M. Nolte, *Chem. Commun.* **1997**, 545–546.

[4] Anthryl-based gelators: a) T. Brotin, R. Utermohlen, F. Fages, H. Bouas-Laurent, J-P. Desvergne, *J. Chem. Soc. Chem. Commun.* **1991**, 416–418; b) M. Lescanne, A. Collin, O. Mondain-Monval, F. Fages, J.-L. Pozzo, *Langmuir* **2003**, *19*, 2013–2020; c) M. Ayabe, T. Kishida, N. Fujita, K. Sada, S. Shinkai, *Org. Biomol. Chem.* **2003**, *1*, 2744–2747.

[5] Urea-based gelators: a) F. S. Schoonbeek, J. van Esch, R. Hulst, R. M. Kellog, B. L. Feringa, *Chem. Eur. J.* **2000**, *6*, 2633–2643; b) C. Shi, Z. Huang, S. Kilic, J. Xu, R. M. Enick, E. J. Beckmann, A. J. Carr, R. E. Melendez, A. D. Hamilton, *Science* **1999**, *286*, 1540–1543; c) J. J. van Gorp, Jef A. J. M. Vekemans, E. W. Meijer, *J. Am. Chem. Soc.* **2002**, *124*, 14759–14769; d) K. Yabuuchi, E. Marfo-Owusu, T. Kato, *Org. Biomol. Chem.* **2003**, *1*, 3464–3469; e) M. de Loos, J. van Esch, R. M. Kellogg, B. L. Feringa, *Angew. Chem.* **2001**, *113*, 633–636; *Angew. Chem. Int. Ed.* **2001**, *40*, 613–616.

[6] Two-component gelators: a) U. Maitra, P. Vijay Kumar, N. Chandra, L. J. D'Souza, M. D. Prasanna, A. R. Raju, *Chem. Commun.* **1999**, 595–596; b) K. S. Partridge, D. K. Smith, G. M. Kykes, P. T. McGrail, *Chem. Commun.* **2001**, 319–320; c) P. Babu, N. M. Sangeetha, P. Vijaykumar, U. Maitra, K. Rissanen, A. R. Raju, *Chem. Eur. J.* **2003**, *9*, 1922–1932; d) S. Kawano, N. Fujita, S. Shinkai, *Chem. Commun.* **2003**, 1352–1353; ion-pair gelators: e) K. Nakano, Y. Hishikawa, K. Sada, M. Miyata, K. Hanabusa, *Chem. Lett.* **2000**, 1170–1171; f) M. Ayabe, T. Kishida, N. Fujita, K. Sada, S. Shinkai, *Org. Biomol. Chem.* **2003**, *1*, 2744–2747; g) R. Oda, I. Huc, S. J. Candau, *Angew. Chem.* **1998**, *110*, 2835–2838; *Angew. Chem. Int. Ed.* **1998**, *37*, 2689–2691.h) D. J. Abdallah, R. G. Weiss, *Chem. Mater.* **2000**, *12*, 406–413, i) M. George, R. G. Weiss, *J. Am. Chem. Soc.* **2001**, *11*, 10393–10394; j) M. George, R. G. Weiss, *Langmuir* **2003**, *19*, 1017–1025.

[7] Amino acid/peptide-based gelators: a) E. J. de Vires, R. M. Kellogg, *J. Chem. Soc. Chem. Commun.* **1993**, 238–240; b) S. Bhattacharya, S. N. Ghanashyam Acharya, A. R. Raju, *Chem. Commun.* **1996**, 2101–2102; c) K. Hanabusa, K. Okui, K. Karaki, T. Koyama, H. Shirai, *J. Chem. Soc. Chem. Commun.* **1992**, 1371–1373; d) K. Hanabusa, Y. Naka, T. Koyama, H. Shirai, *J. Chem. Soc. Chem. Commun.* **1994**, 2683–2684; e) J. Makerević, M. Jokić, L. Frkanec, D. Kalalenić, M. Žinić, *Chem. Commun.* **2002**, 2238–2239; f) H. Ihara, M. Takafuji, T. Sakurai, M. Katsumoto, N. Ushijima, T. Shirosaki, H. Hachisako, *Org. Biomol. Chem.* **2003**, *1*, 3004–3006; g) J. P. Schneider, D. J. Pochan, B. Ozbas, K. Rajagopal, L. Pakstis, J. Kretsinger, *J. Am. Chem. Soc.* **2002**, *124*, 15030–15037; h) M. Suzuki, Y. Nakagima, M. Yumoto, M. Kimura, H. Shirai, K. Hanabusa, *Langmuir* **2003**, *19*, 8622–8624.

[8] a) P. Terech, E. Ostuni, R. G. Weiss, *J. Phys. Chem.* **1996**, *100*, 3759–3766; b) P. Terech, I. Furman, R. G. Weiss, *J. Phys. Chem.* **1995**, *99*, 9558–9566, and references therein.

[9] S. Kobayashi, N. Hamasaki, M. Suzuki, M. Kimura, H. Shirai, K. Hanabusa, *J. Am. Chem. Soc.* **2002**, *124*, 6550–6551.

[10] J. H. Jung, Y, Ono, K. Hanabusa, S. Shinkai, *J. Am. Chem. Soc.* **2000**, *122*, 5008–5009.

[11] W. Kubo, T. Kitamura, K, Hanabusa, Y. Wada, S. Yanagida, *Chem. Commun.* **2002**, 374–375.

[12] a) P. Dastidar, *CrystEngComm* **2000**, 8; b) A. Ballabh, D. R. Trivedi, P. Dastidar, E. Suresh, *CrysEngComm* **2002**, *4*, 135–142; c) D. R. Trivedi, A. Ballabh, P. Dastidar, *CrysEngComm.* **2003**, 5, 358–367.

[13] A. Ballabh, D. R. Trivedi, P. Dastidar, *Chem. Mater.* **2003**, *15*, 2136–2140.

[14] D. R. Trivedi, A. Ballabh, P. Dastidar, *Chem. Mater.* **2003**, *15*, 3971–3973.

[15] S. Bhattacharya, Y. Krishnan-Ghosh, *Chem. Commun.* **2001**, 185–186.

[16] a) R. Luboradzki, O. Gronwald, M. Ikeda, S. Shinkai, D. N. Reinhoudt, *Tetrahedron* **2000**, *56*, 9595–9599; b) S-I. Tamaru, R. Luboradzki, S. Shinkai, *Chem. Lett.* **2001**, 336–337.

[17] K. Biradha, D. Dennis, V. A. MacKinon, C. V. K. Sharma, M. J. Zaworotko, *J. Am. Chem. Soc.* **1998**, *120*, 11894–11903.

[18] C. B. Aakeröy, A. M. Beatty, M. Tremayne, D. M. Rowe, C. C. Seaton, *Cryst. Growth Des.* **2001**, *1*, 377–382.

[19] a) A. Ajayaghosh, S. J. George, *J. Am. Chem. Soc.* **2001**, *123*, 5148–5149; b) A. Ajayaghosh, S. J. George, V. K. Praveen, *Angew. Chem.* **2003**, *115*, 346–349; *Angew. Chem. Int. Ed.* **2003**, *42*, 332–335.

[20] a) W. J. Hehre, L. Radom, P. von. R. Schleyer, *Ab Initio Molecular Orbital Theory*, Wiley, New York, **1986**; TITAN, Wavefunction, Inc, 18401 Von Karman Avenue, Suite 370, Irvine CA 92612 USA; Schrodinger, Inc., 1500 SW First Avenue, Suite 1180, Portland, OR 97201 USA.

[21] CAD-4 Software, Version 5.0; Enraf-Nonius: Delft, **1989**.

[22] I. Gabe, Y. Le Page, I. P. Charland, F. L. Lee, P. S. White, *J. Appl. Crystallogr.* **1989**, *22*, 384–387.

[23] Sheldrick, G. M. SHELEXL-97, A program for crystal structure solution and refinement, University of Göttingen, Göttingen (Germany), **1993**.

[24] A. L. Spek, PLATON-97, University of Utrecht (The Netherlands), **1997**.

[25] Mercury 1.1.1 Supplied with Cambridge Structural Database, Copyright CCDC, **2001–2002**.

[26] a) G. R. Desiraju, *Angew. Chem.* **1995**, *107*, 2541–2558; *Angew. Chem. Int. Ed.* **1995**, *34*, 2311–2327; b) J. N. Moorthy, R. Natarajan, P. Mal, P. Venugopalan, *J. Am. Chem. Soc.* **2002**, *124*, 6530–6531.

Received: February 6, 2004
Published online: September 20, 2004

